Replication of photonic crystals by soft ultraviolet-nanoimprint lithography

Michele Belotti, Jérémi Torres,[a] Emanuel Roy, Anne Pépin, and Yong Chen[b]
Laboratoire de Photonique et Nanostructures, Route de Nozay, 91460 Marcoussis, France

Dario Gerace and Lucio Claudio Andreani
Dipartimento di Fisica "A. Volta," Università degli Studi di Pavia, via Bassi 6, 27100 Pavia, Italy

Matteo Galli
Instituto Nazionale di Fisica della Materia, via Bassi 6, 27100 Pavia, Italy

(Received 26 July 2005; accepted 1 December 2005; published online 24 January 2006)

Nanoimprint lithography assisted by ultraviolet photopolymerization through a soft elastomer-based mold is applied to the fabrication of silicon-on-insulator slab photonic crystals for optical wavelengths. Variable angular reflectance is used to measure the dispersion of the photonic leaky modes. Experimental results are in good agreement with both theoretical calculations and previous results obtained by standard nanoimprint lithography as well as conventional nanofabrication techniques such as electron-beam lithography. © *2006 American Institute of Physics*. [DOI: 10.1063/1.2159544]

I. INTRODUCTION

Nanolithography is finding increasing application in the field of optoelectronics and nanophotonics. One promising application lies in the fabrication of photonic structures with optical subwavelength periodicity such as two-dimensional photonic crystals (PhCs).[1–4] Periodically patterned planar waveguides are indeed suited to control light behavior in quasi three-dimensional (3D) structures. By embedding a two-dimensional photonic lattice in a slab waveguide between lower index claddings, light confinement in the third direction is provided. These structures exhibit remarkable optical properties related to the strong modulation of electromagnetic waves, such as optical guiding obtained by the introduction of linear defects in the periodicity. Guiding occurs along the defect line, i.e., a missing row of holes forming the so-called W1 defect.[5] In order to enhance this behavior, high dielectric contrast between core and claddings is required. For this reason and also for complete compatibility with complementary metal-oxide-semiconductor (CMOS) materials and processes, silicon-on-insulator (SOI) patterned waveguides are ideal candidates for realizing planar-integrated photonic devices.

The commonly used technique for the fabrication of PhCs for optical wavelength range is based on electron-beam lithography (EBL).[6] Although EBL is a powerful high-resolution nanolithography technique, it is expensive and time consuming due to its direct write scanning beam operation, and therefore not suitable for mass production. Alternatively, low-cost emerging nanolithography techniques have been investigated. In particular, nanoimprint lithography,[7–9] (NIL) has shown to be a cost-effective high-resolution replication method compatible with conventional pattern transfer techniques and was efficiently applied to PhC fabrication.[10,11] However, the NIL process is based on hot embossing of plastic polymers at high temperature and under high pressure which are not suitable for a number of applications. More recently, UV light-assisted NIL (UV-NIL) or step-and-flash imprint lithography,[12] (SFIL) has been developed which overcomes both the speed limitations due to the heating cycle and high pressure and the overlay restraints of standard NIL. In UV-NIL, a UV-transparent hard material template (typically quartz) is used to imprint a low-viscosity UV-curable prepolymer solution, which can be photopolymerized under UV exposure through the mold, at room temperature and under very low pressure. High-resolution patterns can be defined over a large surface by step and repeat imprinting, and optical alignment is also enabled. However, to our knowledge SFIL has never been applied to PhCs fabrication. Recently, a new approach, named soft UV-NIL, based on the use of soft material templates, was proposed for single-step large area pattern replication.[13] A transparent silicone elastomer of low Young's modulus, polydimethylsiloxane (PDMS), is used for the fabrication by cast molding of soft molds ensuring conformal contact with large surfaces. Such an approach is attractive because of its simplicity, low cost, and high throughput. However, the resolution achievable with a single-layer PDMS stamp is limited due to deformation of the elastomeric pattern. As an example, PDMS deformation can induce a variation in the width of high-resolution defects changing drastically the optical properties of such PhCs waveguides. More recently[14] we proposed a new trilayer stamp configuration which introduce a thin film of harder plastic material at the surface of the PDMS mold in order to reduce local deformation when stamping while ensuring single-step large area imprint.

In this paper, we report on the successful application of this innovative technique for the fabrication of two-dimensional PhCs in commercial SOI. The choice of material and spectral range is motivated by the integration of optical functions within silicon microelectronic chips and telecommunication application potentialities.

[a]Electronic mail: torres@cem2.univ-montp2.fr
[b]Also at Ecole Normale Superieure, 24 rue Lhomond, 75005 Paris.

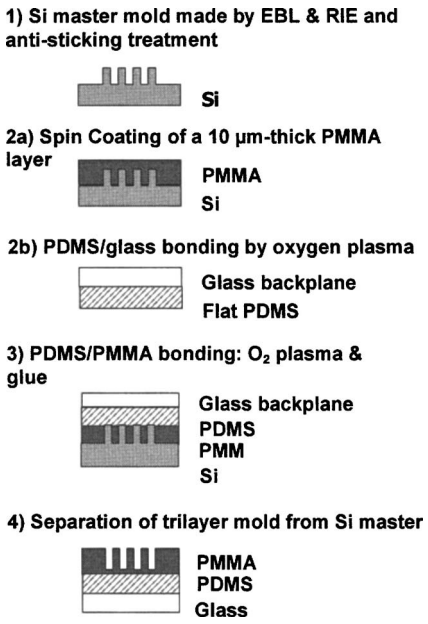

FIG. 1. Trilayer stamp fabrication process. (1) The silicon master is realized by high-resolution electron-beam lithography and is treated with TMCS by chemical-vapor deposition. (2) (a) A 10-μm-thick PMMA layer is spin coated onto the Si master. (b) The back surface of the PDMS buffer and glass slide are treated with an oxygen plasma before bonding them irreversibly. (3) PDMS is bonded onto the PMMA layer using an oxygen plasma and cyanoacrylate glue. (4) Glass/PDMS/PMMA assembly is separated from the Si master.

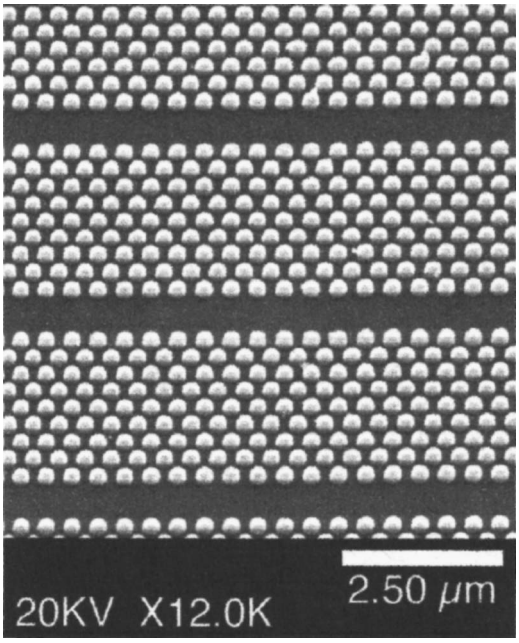

FIG. 2. Scanning electron micrograph of the silicon master containing a two-dimensional array of pillars: diameter 200 nm, periodicity 400 nm, and etch depth 250 nm. A line of pillars is missing each five periods in order to create a line of defects.

II. FABRICATION

Figure 1 describes the successive steps in the trilayer mold fabrication. The silicon master mold is fabricated by high-resolution EBL using a JEOL JBX5D2U vector scan electron-beam generator operating at 50 keV on a 150-nm-thick poly(methylmethacrylate) (PMMA) resist layer. A 20-nm-thick film of Ni is deposited after resist development. After lift-off, patterns were transferred into silicon by anisotropic SF_6/CHF_3 reactive ion etching (RIE) in a Nextral NE 110 reactor with an etch depth of 250 nm. The pattern, made by EBL, is typically a triangular two-dimensional array of 200 nm diameter pillars with a periodicity of $a=400$ nm, displayed on the scanning electron micrograph (SEM) of Fig. 2. A line of pillars is missing each five periods in order to create a W1 line defects with supercell periodicity $d=5\sqrt{3}a$ along the ΓM direction of the PhC which is perpendicular to the defect direction.[15] The width of defects can also be modulated in order to modify the optical properties of the PhC waveguide. The surface of the fabricated silicon mold is then treated with tri(chloromethylsiloxane) (TMCS), by chemical-vapor deposition, which forms a self-assembling monolayer for antiadhesion.

The next step is the realization of the thin plastic imprinting layer of the trilayer stamp. We chose the PMMA, a thermoplastic polymer of Young's modulus $E=5.2$ GPa, to achieve this purpose. A 10 μm thick of such a PMMA layer is spin coated on the silicon master and post baked for complete solvent evaporation. In parallel, the PDMS ($E=0.75$ MPa) buffer layer is obtained by casting a liquid prepolymer mixed with a cross-linking agent (commercially available GE RTV615 kit) on a flat unpatterned Si wafer and curing it at 80 °C for 1 h. The PDMS top surface is then irreversibly bonded to a glass slide by an oxygen plasma treatment. The PDMS bottom surface is then bonded to the PMMA layer with the help of cyanoacrylate glue. After 1 h at 80 °C, the (glass backplane/PDMS buffer/patterned PMMA layer) assembly can be separated from the silicon master. All mold materials are transparent in the 250–900 nm range.

For our soft UV-NIL process, illustrated in Fig. 3(a), a bilayer resist system was used in order to obtain resist pat-

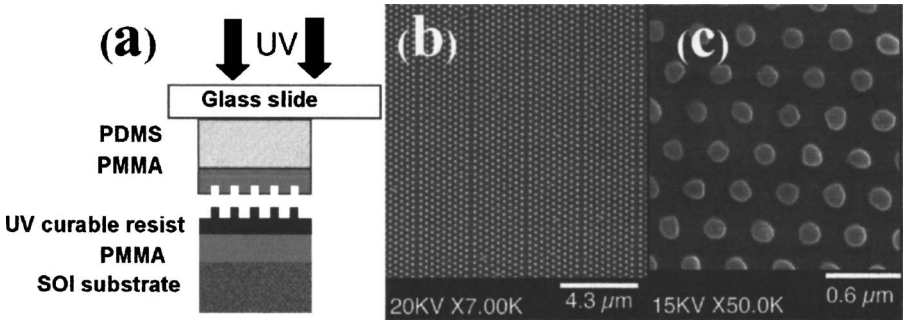

FIG. 3. (a) Schematic representation of the soft UV-NIL process. The trilayer stamp is lightly pressed into the NXR 2030 UV-curable liquid resist and UV exposed at room temperature. (b) The pattern is transferred in the PMMA layer by oxygen plasma using NXR 2030 resist as etching mask. (c) Zoom of (b) for clearer view of the transferred pattern.

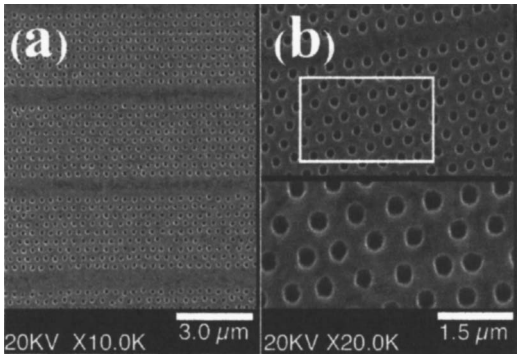

FIG. 4. (a) Scanning electron micrograph of the imprint after Ni lift-off in warm trichloetylene. Ni is used as a mask for transfer in the SOI substrate. (b) Scanning electron micrograph of the soft UV-imprinted two-dimensional PhC after Ni mask removal. The pattern comprises 180 nm diameter holes with a periodicity of $a=400$ nm and an etch depth of 250 nm. The supercell periodicity $d=5\sqrt{3}a$ is clearly visible and contains the W1 defect mode.

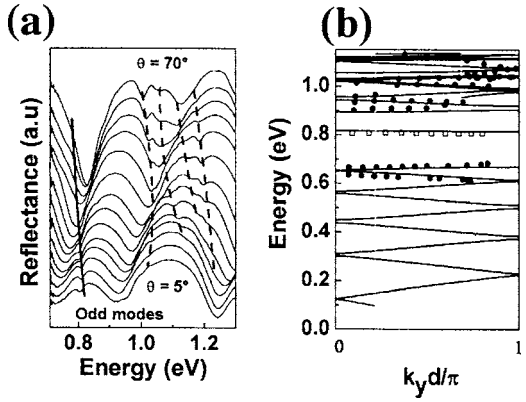

FIG. 5. Reflectance measurements along the ΓM orientation for the TE polarization on the PhC fabricated by soft UV-NIL and subsequent RIE. (a) The curves are vertically shifted for clarity. Curves from 5° to 70° with a 5° step are shown. Dashed curves indicate the position of the bulk mode resonances whereas the defect mode is indicated by a solid line. (b) Corresponding photonic bands folded into the reduced Brillouin zone due to supercell periodicity: experiments (empty squares for defect mode; filled circles for bulk modes) and theory (solid lines).

terns with high aspect ratio and thus facilitate the metal lift off used for the pattern transfer into SOI. The bottom resist layer is a 200-nm-thick PMMA layer spin coated on the SOI substrate. A UV-curable organosilicon, with low viscosity, prepolymer NXR 2030 developed by Nanonex, is then spin coated over the PMMA layer. That top layer is used as the imprint resist. The soft UV-NIL process was carried out at an ultralow imprint pressure of 0.05 bar, under UV exposure at an intensity of 60 mW/cm^2, and for 150 s [Fig. 3(a)]. After separation, the NXR 2030 residual layer and the underlying PMMA were etched by oxygen plasma RIE [see Figs. 3(b) and 3(c)] down to the SOI substrate, using the patterned NXR 2030 resist as an etch mask with selectivity close to 20 with respect to PMMA. A thin Ni layer is then evaporated onto the resist surface and lifted off by dissolution of PMMA in warm trichloroethylene, giving the structure shown in Fig. 4(a).

The Ni is then used as a mask for a second RIE step to etch the silicon top layer of the SOI structure, consisting in a 260-nm-thick silicon core on a 1-μm-thick SiO_2 cladding layer grown on a silicon substrate. A mixture with a SF_6 of 4 SCCM (standard cubic centimeter per minute) gas flow rate and CHF_3 of 8 SCCM gas flow rate at a 10 mT pressure and rf power of 15 W is used. The etching rate is typically 50 nm/min and RIE parameters are optimized to obtain nearly vertical sidewalls. Finally, the remaining Ni mask is removed in a 10% nitric acid solution. The achieved PhC structure is displayed in Fig. 4(b).

The final structure obtained by soft UV-NIL and subsequent RIE is a two-dimensional PhC slab of 180 nm diameter holes with a triangular periodicity of 400 nm and an etch depth of 250 nm. The defect line that appears each five periods is clearly visible.

III. RESULTS AND DISCUSSION

As can be seen in Fig. 4(b), a homogeneous imprinting is achieved, with a limited variation of the holes diameter $<15\%$ on a 200×200 μm^2 area. The use of a trilayer mold produces an high-fidelity replication with a variation of the structures size (diameter) from 200 nm (Si mold) to 180 nm (PhC) due to NXR 2030 mask under etching during the oxygen RIE. For performance comparison, we have probed the photonic optical properties of our soft UV-nanoimprinted PhCs through optical characterization. The optical response of the sample in the radiative region, i.e., above the light line, has been probed by means of angle-resolved specular reflectance from the sample surface. The optical setup, inspired from that proposed by Astratov *et al.*,[16] is used for the determination of the photonic band dispersion of SOI-based PhCs. It relies on the observation of the coupling between the incoming beam and photonic modes in the periodically patterned slab, which gives rise to resonant features in the optical spectra. The evolution of these features as a function of incidence angle leads to a determination of the in-plane wave vector at a given frequency. The detail of this technique has been reported elsewhere.[17]

In Fig. 5(a) we display the variable angle reflectance spectra of our soft UV-NIL-fabricated PhC sample along the ΓM direction for a TE polarized incident light. The angle of incidence is varied from 5° to 70° with a 5° step. The curves are shifted by an arbitrary quantity in order to facilitate viewing. The curves display a prominent interference pattern due to multiple interference occurring at the core-cladding and cladding-substrate interfaces of the SOI guide. Superimposed to the interference fringes, several sharp features that mark the excitation of photonic modes are clearly visible in the spectra. Similar spectra were obtained on PhCs realized by high-resolution EBL.[15–19] While bulk resonances (dashed curves) are characterized by strong dispersions as a function of the angle of incidence, the defect mode (solid line) is dispersionless at about 0.8 eV.[15] The width of these resonances is much smaller than that obtained from PhCs realized by standard NIL, and roughly the same as EBL-made PhCs.[10,15] These results demonstrate the high quality of our trilayer stamp soft UV-NIL approach.

A plot of the energy positions of the resonances as a function of the in-plane wave vector along the ΓM direction of symmetry is given in the diagrams of Fig. 5(b). Filled

circles (empty squares) correspond to the energy dispersion of the photonic bulk modes (defect mode). Theoretical curves are obtained by a method that we have recently reported,[20] in which the magnetic field is expanded onto the basis consisting of the guided modes of a homogeneous air/Si/SiO_2 waveguide. The dielectric constant in the core layer is taken to have an average value. The equation for the magnetic field is transformed into a linear eigenvalue problem which is solved by numerical diagonalization. A supercell approach is used to take into account the defect periodicity. Taking the origin of the z axis in the middle of the slab, specular reflection with respect to the (x,y) plane is a symmetry operation. We consider here only odd bulk modes $(\sigma_{xy}=+1)$ along the ΓM direction of symmetry because in this direction these modes show a photonic band gap between 0.67 and 0.86 eV in which the defect appears. In addition, defect mode is classified according to reflection symmetry $\sigma_{kz}=\pm 1$ with respect to the plane bisecting the channel. Only odd defect mode $(\sigma_{kz}=+1)$ along ΓM direction is represented in Fig. 5. Notice that the modes are folded into a reduced Brillouin zone $(-\pi/d;\pi/d)$ due to the supercell periodicity.[15] Very good agreement is found by comparing the curves obtained by the extraction of the experimental resonance energies and the theoretically calculated ones [circles and squares versus solid lines in Fig. 5(b)]. This comparison proves the ability of soft UV-NIL to produce high-quality photonic crystal slabs with or without defects.

IV. CONCLUSIONS

In conclusion, we have demonstrated the fabrication of two-dimensional PhCs for optical wavelengths by an innovative nonconventional nanofabrication technique, soft UV-NIL using trilayer molds. Variable angular reflectance has been used to measure the dispersion of the leaky photonic modes of the system, showing very good agreement with numerical modeling results. Soft UV-NIL therefore appears as a simple, low-cost, fast-operation, imprint-based nanolithography technique, compatible with conventional pattern transfer techniques.

We would like to mention that one of the motivations of developing soft UV-NIL is to apply such a technique to a variety of semiconductor materials, such as GaAs, InP, and GaN, which are classically used for optoelectronics applications. Our previous experiences have shown that it is quite difficult to apply thermal NIL techniques on delicate materials because of the relative high-applied pressure (GaAs and InP wafers are much fragile than Si wafers). With the soft UV-NIL technique demonstrated in this work, it should be possible to work not only with fragile samples but also to avoid the possible degradations of the sample's quality due to thermal processes.

ACKNOWLEDGMENTS

This work was partly supported by the European Commission through Research Projects SOUVENIR (IST-2001-37472) and NaPa (IST500120).

[1] E. Yablonovitch, Phys. Rev. Lett. **58**, 2059 (1987).
[2] S. John, Phys. Rev. Lett. **58**, 2486 (1987).
[3] K. Sakoda, *Optical Properties of Photonic Crystals* (Springer, Berlin, 2001).
[4] S. G. Johnson and J. D. Joannopoulos, *Photonic Crystals: The Road from Theory to Practice* (Kluwer, Dordrecht, 2002).
[5] S. G. Johnson, P. R. Villeneuve, S. Fan, and J. D. Joannopoulos, Phys. Rev. B **62**, 8212 (2000).
[6] D. Peyrade *et al.*, Microelectron. Eng. **61–62**, 529 (2002).
[7] S. Y. Chou, P. R. Krauss, and P. J. Renstrom, Science **272**, 85 (1996).
[8] S. Zankovych, T. Hoffmann, J. Seekamp, J.-U. Bruch, and C. M. Sotomayor Torres, Nanotechnology **12**, 91 (2001).
[9] J. Haisma, M. Verheijen, K. Heuvel, and J. Berg, J. Vac. Sci. Technol. B **14**, 4124 (1996).
[10] M. Belotti, M. Galli, D. Bajoni, L. C. Andreani, G. Guizzetti, D. Decanini, and Y. Chen, Microelectron. Eng. **73–74**, 405 (2004).
[11] A. Chen, S. J. Chua, C. G. Fonstad, B. Wang, and O. Wilhelmi, Advanced Materials for Micro-and Nano-Systems (2005).
[12] M. Colburn *et al.*, Proc. SPIE **3676**, 379 (1999).
[13] U. Plachetka, M. Bender, A. Fuchs, B. Vratzov, T. Glinsner, F. Lindner, and H. Kurz, Microelectron. Eng. **73–74**, 167 (2004).
[14] E. Roy, Y. Kanamori, M. Belotti, and Y. Chen, Microelectron. Eng. **78–79**, 689 (2005).
[15] M. Galli, M. Belotti, D. Bajoni, M. Patrini, G. Guizzetti, D. Gerace, M. Agio, L. C. Andreani, and Y. Chen, Phys. Rev. B **70**, 081307 (2004).
[16] V. Astratov, M. Skolnick, S. Brand, D. Z. Karimov, R. M. Stevenson, D. Whittaker, and I. Culshaw, IEE Proc.: Optoelectron. **145**, 398 (1998).
[17] M. Galli *et al.*, Phys. Rev. B **65**, 1 (2002).
[18] V. Pacradouni, W. Mandeville, A. Cowan, P. Paddon, J. Young, and S. R. Johnson, Phys. Rev. B **62**, 4204 (2000).
[19] D. Coquillat *et al.*, Opt. Express **12**, 1097 (2004).
[20] L. C. Andreani and M. Agio, IEEE J. Quantum Electron. **38**, 891 (2002).